ELSEVIER

Journal of Organometallic Chemistry 641 (2002) 15–25

Journal of Organometallic Chemistry

www.elsevier.com/locate/jorganchem

Electronic coupling in covalently-linked M–M quadruple bonds: $M_2\delta$ to ligand π conjugation☆

Malcolm H. Chisholm *

3144 Newman and Wolfrom Laboratories, Department of Chemistry, The Ohio State University, 100 W. 18th Avenue, Columbus, OH 43210-1185, USA

Received 26 April 2001

Abstract

Dimetal tetracarboxylates, $M_2(O_2CR)_4$, where R = alkyl and M = Mo or W, can be linked in a perpendicular or parallel manner through the agency of a variety of ligands to give 'dimers of dimers' $[M_2(O_2CR)_3]_2$(bridge), or extended chains. A ring of formula $[M_2(O_2CR)_2(\text{bridge})]_4$ is an alternative to a chain $[M_2(O_2CR)_3]_2(\text{bridge})_2]_\infty$ and 'molecular squares' of formula $[(RNCHNR)_2M_2(\text{bridge})]_4$ have recently been reported by Cotton and Murillo, where M = Mo and Rh and R = *p*-$MeOC_6H_4$. The electronic coupling between the M_2 units manifests itself in electrochemical data and in the electronic spectra of the compounds. The electronic coupling occurs by $M_2\delta$ to ligand π-conjugation and specific examples are illustrated for the bridging ligands oxalate, perfluoroteraphthalate, 1,8-anthracenedicarboxylate and 2,7-dioxynaphthyridine. Correlations of a variety of spectroscopic data and computations employing density functional theory are presented.

Keywords: Electonic coupling; Spectra; Ligands

1. Introduction

In this article, I review briefly the work that was started in my laboratory by Dr Roger Cayton some 10 years ago and present some ongoing unpublished work which reveals the wealth of chemistry that remains to be explored. The idea was a simple one. Let us see if we can link M–M multiple bonded complexes together to form polymers of the type shown in **I** and **II** below. We referred to these as perpendicular and parallel polymers, respectively, a nomenclature based on the relative orientation of the M–M axis with respect to the linear polymer chain.

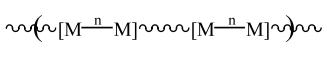

I

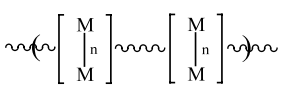

II

As a starting point, Dr Cayton took the $M_2(O_2CR)_4$ compounds, where M = Mo or W, as the building blocks since these compounds could be readily made in gram quantities and their electronic structures had been extensively investigated [1]. The d^4–d^4 dinuclear compounds adopt a paddlewheel or lantern-type structure in the solid-state and are weakly bonded to their neighboring molecules through the agency of long dative O-to-M bonds as shown in **III**.

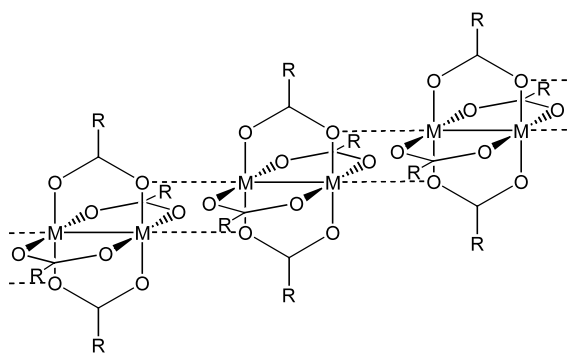

III

The M–M bond is a quadruple bond of configuration $\sigma^2\pi^4\delta^2$ and readily undergoes a one-electron oxidation. This occurs much more easily for M = W and the

☆ Based on a talk in the International Symposium 'Extended π-Systems', Heidelberg, April 2001.

* Corresponding author.

E-mail address: chisholm@chemistry.ohio-state.edu (M.H. Chisholm).

0022-328X/02/$ - see front matter
PII: S0022-328X(01)01365-1

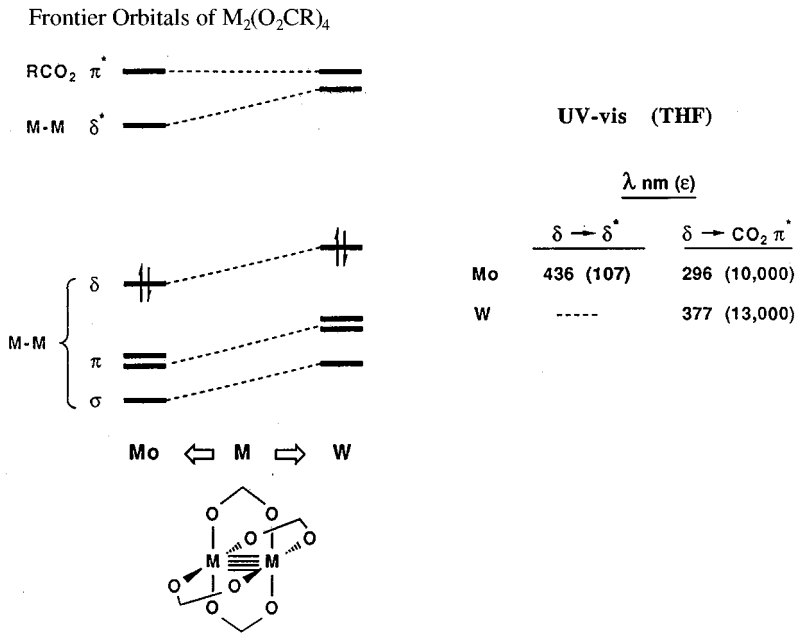

Fig. 1. Comparison of the energies of the frontier molecular orbitals in $M_2(O_2CR)_4$ compounds, where M = Mo and W.

frontier MO diagram comparing the two metals in $M_2(O_2CR)_4$ compounds is shown in Fig. 1. For M = Mo, the singlet δ–δ* transition is visible in the electronic spectrum as a weak band at $\lambda_{max} \sim 460$ nm ($\varepsilon \sim 100\ M^{-1}\ cm^{-1}$) but for M = W, this is masked by the fully allowed δ to O_2C π* transition which is red shifted in comparison to its molybdenum analogue. If R = Ph or *p*-$NO_2C_6H_4$, this δ to CO_2 π* transition can be shifted to lower energy in the visible region of the spectrum [2].

Since $M_2(O_2CR)_4$ compounds are substitutionally labile, two simple routes to polymers of types I and II were explored [3]. The first involved the carboxylate exchange reaction represented by Eq. (1).

$$M_2(O_2CR)_4 + HO_2C(X)CO_2H \rightarrow [M_2(O_2CR)_2(O_2CXCO_2)] + 2RCO_2H \quad (1)$$

The second involved a metathesis reaction employing the solvento complexes $[M_2(O_2CR)_2(CH_3CN)_4]^{2+}[BF_4^-]_2$ (Eq. (2)).

$$[M_2(O_2CR)_2(CH_4CN)_4]^{2+}[BF_4^-]_2 + 2Na^+[bridge^{2-}] \rightarrow [M_2(O_2CR)_2(bridge^{2-})] + 2NaBF_4 \quad (2)$$

We encountered problems right away! As the reader may have anticipated, the desired products in Eqs. (1) and (2) were insoluble and intractable. Moreover, Eq. (1) is an equilibrium reaction and has to be driven to the right either by thermodynamic factors or by removing RCOOH. To compound matters further, the complexes are kinetically labile to ligand exchange which may be brought about by adventitious H^+ or carboxylate$^-$ [4]. There was, however, no doubt that we were on the right track and some oligomeric species were soluble in solvents such as THF or CH_3CN. In an attempt to simplify matters, we determined to prepare 'dimers of dimers' by modifying reactions (1)–(4), respectively.

$$2[M_2(O_2CR)_4] + H_2OCXCO_2H \rightarrow [M_2(O_2CR)_2]_2(O_2CXCO_2) + 2RCOOH \quad (3)$$

$$2[M_2(O_2CR)_3(CH_3CN)_2]^+BF_4^- + 2Na^+(bridge^{2-}) \rightarrow [M_2(O_2CR)_3]_2(bridge^{2-}) + 2NaBF_4 \quad (4)$$

Several bridging dicarboxylates were employed and several 'dimers of dimers' were characterized. The reader should note that many similar compounds have

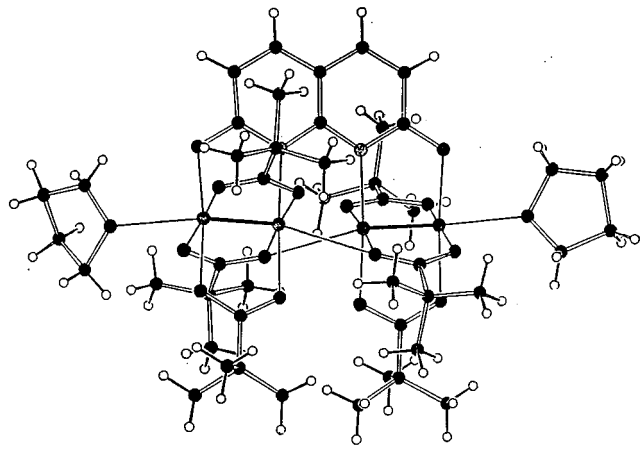

Fig. 2. A drawing of the $[Mo_2(O_2CCMe_3)_3]_2$(μ-2,7-dioxynaphthyridine)-2THF molecule.

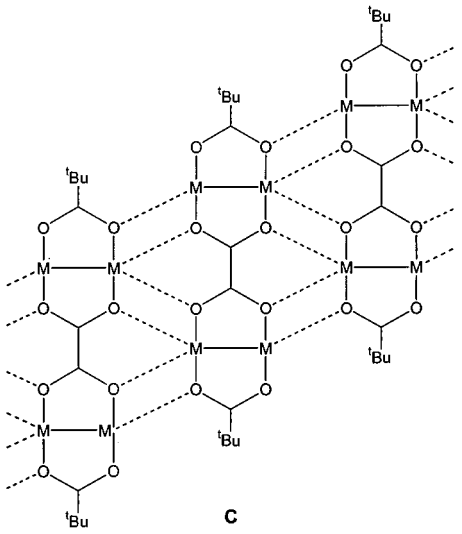

Fig. 3. A drawing of the extended chain structure showing the M···O linkages in the solid-state structure of $[Mo_2(O_2CCMe_3)_3]_2(\mu\text{-}O_2CCO_2)_\infty$.

recently been prepared by Cotton and Murillo and coworkers employing formamidinate attendant ligands $[(RNCHNR)_3Mo_2]_2$(bridge), where the bridge is a dicarboxylate, and at least twelve have been structurally characterized [5–7]. Of the near score or so compounds prepared by Cayton, he was only able to obtain single crystals of one that were suitable for a single crystal X-ray diffraction study.

The structure of the 2,7-dioxynaphthyridine bridged pivalate is shown in Fig. 2. A slight ruffling of the planar fused six-membered rings allows for the avoidance of otherwise very short O–O distances and even allows for favorable weak Mo_2···O bond formation of the type seen in the $M_2(O_2CR)_4$ compounds as shown in **III**. The terminal Mo atoms of the Mo_4 chains are bonded to THF molecules. In toluene-d_8 solution at 25 °C, the molecule has a time-averaged mirror plane as only two types of ^{t}Bu groups are visible in the ^{1}H-NMR spectrum but on cooling to −80 °C, one observes three ^{t}Bu singlets of equal integral intensity consistent with the C_2 symmetry found in the solid-state [3].

The 1,8-anthracenedicarboxylate compound adopts a related structure though it is not necessary for the anthracene rings to ruffle since there is free rotation about the ring C to carboxylate C bond. The reader should note that 2,7-dioxynaphthyridine and 1,8-anthracene carboxylate ligands may be viewed as stereochemically correspondent in the arrangement of the four metal atoms in a chain. This is easily seen by an inspection of the drawing of the ligands in **IV** and **V**. Thus the central M to M distance in these molecules is ca. 3.0 Å, as seen in Fig. 2.

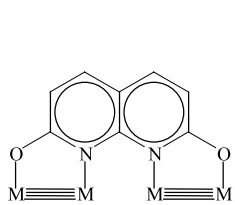

IV

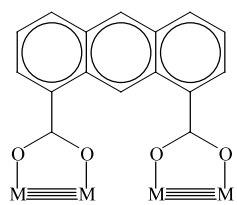

V

From spectroscopic studies and from elemental analyses, there was little doubt that Cayton had made compounds of the type $[M_2(O_2C^tBu)_3]_2(\text{-}O_2CXCO_2)$. The comparison of 1:12 crystal structures in favor of the Texas group is an unfair reflection of Cayton's crystal growing skills since Cotton and Murillo's 'dimers of dimers' are actually discrete molecules in the solid-state [5–7]. The carboxylates form extended lattice structures as a result of forming weak intermolecular interactions involving the axial sites of the metal atoms. When this happens, crystals are often either thin plates or long thin hairs.

Table 1
Summary of selected electrochemical data for bridged compounds $[(^tBuCO_2)_3M_2]_2$(bridge)

Compound		$\Delta E_{1/2}$ (mV) [a]	K_c [b]	Class [c]
Metal	Bridge			
Mo	Oxalate	280	5.4×10^4	**II**
W	Oxalate	717	1.3×10^{12}	**III**
Mo	Perfluoroterephthalate	65	13	**I**
W	Perfluoroterephthalate	285	6.6×10^4	**II**
Mo	9,10-Dihydro 1,8-anthracene dicarboxylate	106	62	**I**
W	9,10-Dihydro 1,8-anthracene dicarboxylate	146	2.9×10^2	**I** or **II**
W	1,8-Anthracenedicarboxylate	156	4.3×10^2	**I** or **II**
Mo	1,7-Dioxynaphthyridine	389	3.8×10^6	**II** or **III**

Data from ref. [3].
[a] $\Delta E_{1/2} = E^2_{1/2} - E^1_{1/2}$.
[b] K_c, comproportionation constant for the reaction $[M_2]_2(\text{bridge}) + [M_2]_2\text{bridge}^{2+} \rightleftharpoons 2[M_2]_2(\text{bridge})^+$.
[c] Class **I**, valence trapped; Class **III**, fully delocalized, from Ref. [10].

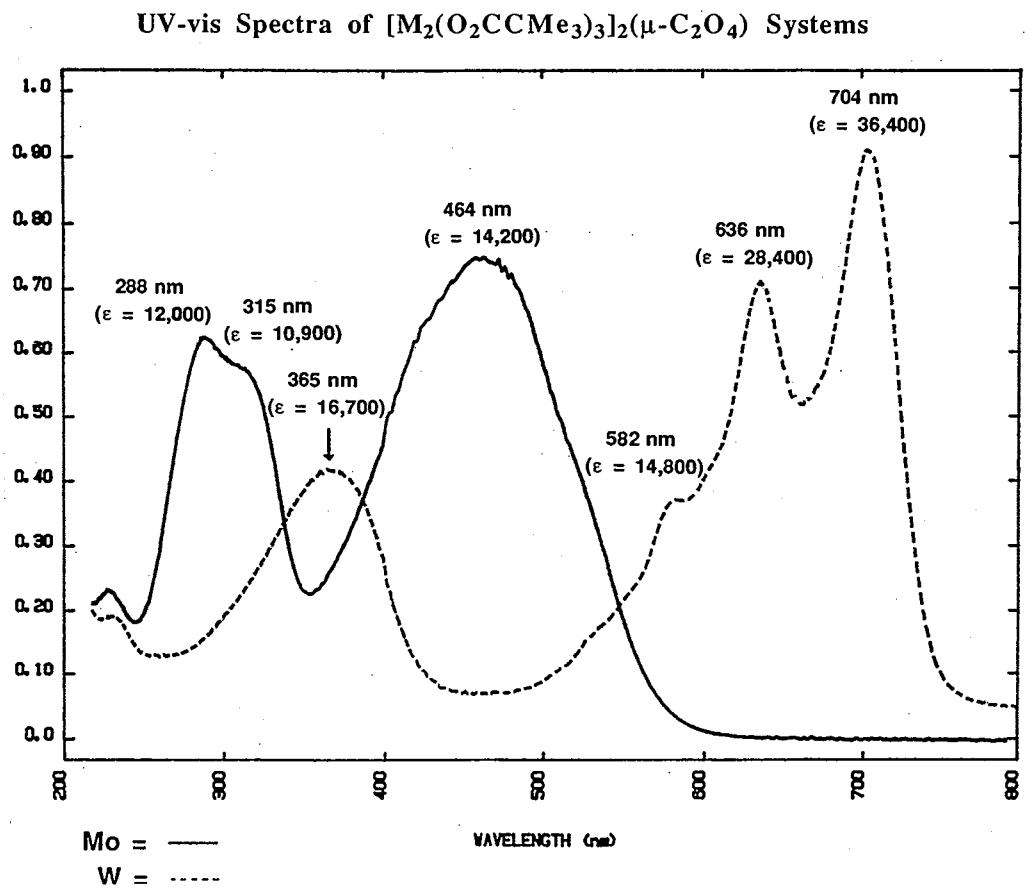

Fig. 4. UV–vis spectra of $[M_2(O_2CCMe_3)_3]_2(\mu\text{-}O_2CCO_2)$, where M = Mo and W, recorded at room temperature in THF.

Dr Paul Wilson, a current postdoctoral associate, has revisited this problem and, in collaboration with a colleague, Patrick Woodward, is attempting to solve these molecular structures by a combination of X-ray powder patterns and solid-state NMR techniques. At this time, we think we have sorted out the solid-state molecular structure of the oxalate bridged compound $[(^tBuCO_2)_3Mo_2]_2(\mu\text{-}O_2CCO_2)$. From ^{13}C labeling of the oxalate carbons, we have just one ^{13}C oxalate carbon signal. From indexing X-ray data sets obtained with various λ, we can determine the space group and the cell dimensions. Then employing the metrical parameters for the hypothetical molecule $[(HCO_2)_3Mo_2]_2(\mu\text{-}O_2CCO_2)$ obtained from density functional theory, we can build the pivalate molecule by replacing the C–H bonds by C–^{t}Bu groups. We introduce this into the unit cell and by modeling programs fit (simulate) the observed diffraction data. Although this method will not generate very accurate bond distances, certainly not when compared with single crystal data structure solutions, we obtain reliable information about the overall packing of the molecule. The structure involves infinite Mo_4(μ-oxalate) chains as shown in Fig. 3 [8]. The central $Mo_2(\mu\text{-}O_2CCO_2)Mo_2$ unit is nearly planar as we had anticipated from the electronic spectra of the compound recorded in a mull (vide infra) [9].

We are hoping to be able to solve several related structures involving different bridging groups by similar techniques. For example, the structure of the related $\mu\text{-}O_2C\text{–}C_6F_4\text{–}CO_2$ compound is also microcrystalline but the electronic spectra recorded in a mull leads us to believe that the two Mo_2 units linked by the perfluoroteraphthalate are not in a plane (vide infra).

Electrochemical studies, particularly those employing cyclic voltammetry provide evidence of the electronic coupling between the M_2 centers [3]. Examples of class **I**, **II** and **III** mixed valence compounds can be formed depending upon the bridge [10]. For a related pair of compounds, the coupling is notably stronger for tungsten relative to molybdenum, a trend that parallels coupling between metal centers in $[(NH_3)_5M(\text{bridge})\text{-}M(NH_3)_5]^{5+}$ compounds where M = Ru or Os [11]. This is a result of the combined influence of the greater effective radial extension of the 5d orbitals from the core and orbital energies which favor d_π to ligand π^* bonding for the third row element. Representative electrochemical data are given in Table 1. The poor coupling between the Mo_2 centers in the anthracene dicarboxylate bears testimony to the importance of $M_2\delta$ to ligand π^* coupling since the central Mo–Mo distance can not be much greater than 3.1 Å.

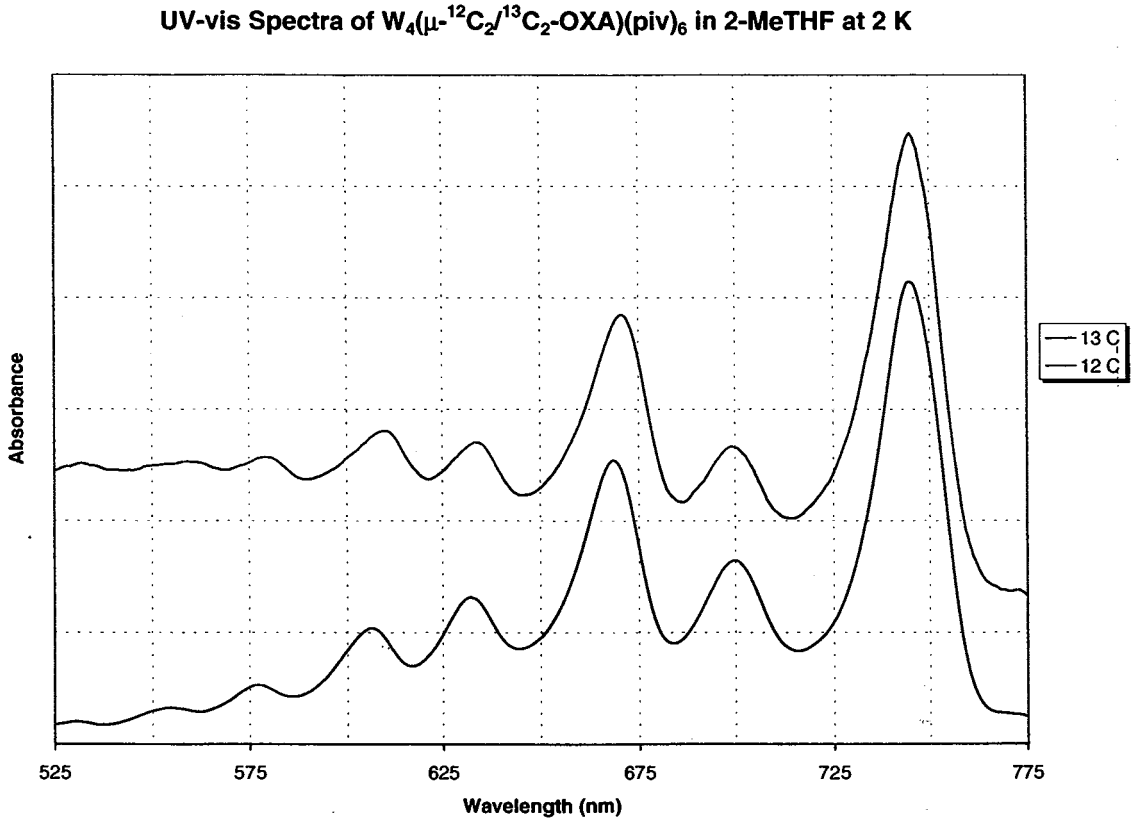

Fig. 5. Comparison of the ^{12}C (bottom) and ^{13}C labeled oxalate visible spectrum (top) of $[W_2(O_2CCMe_3)_3]_2$ (μ-$O_2^*C^*CO_2$) recorded in 2-MeTHF at 2 K.

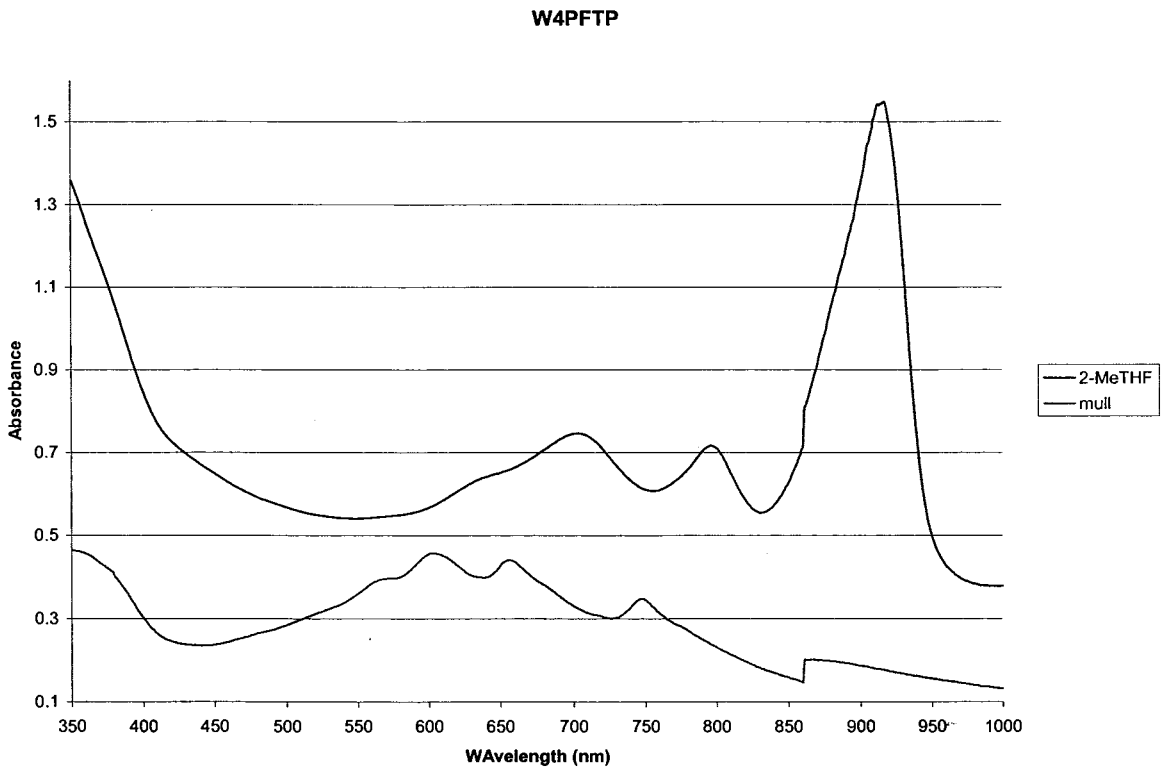

Fig. 6. Comparison of the room temperature solution (2-MeTHF) and mull electronic spectrum of $[W_2(O_2CCMe_3)_3]_2(\mu\text{-}O_2CC_6F_4CO_2)$. The sharp rise/fall at ca. 860 nm is an instrumental glitch.

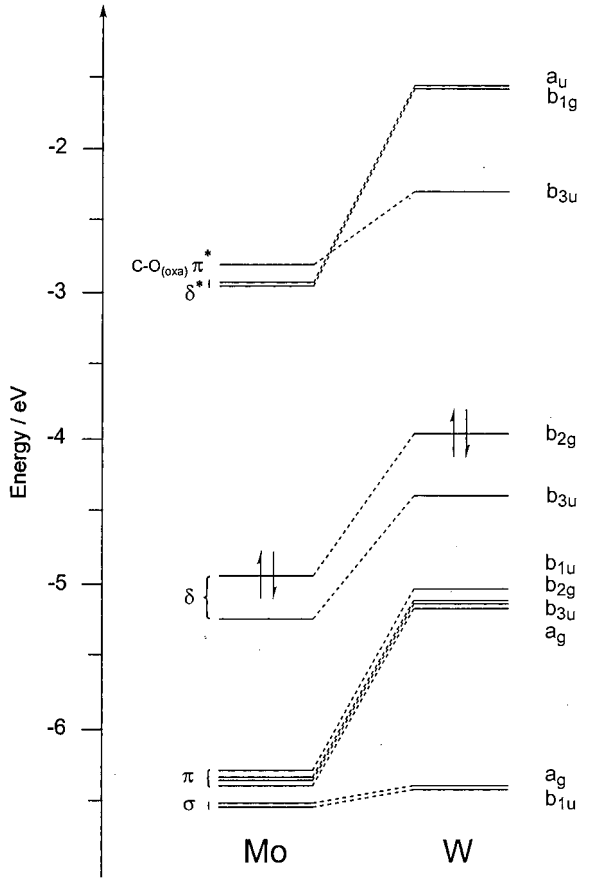

Fig. 7. Comparison of the frontier molecular orbital energies calculated for the $[M_2(O_2CH)_3]_2$ (μ-O_2CCO_2) molecules, where M = Mo and W.

Cotton and Murillo in their recent study of $[(RNCHNR)_3Mo_2]_2$(bridge) compounds noted similar findings and noted how the coupling falls off with increasing distance (length of the bridge) [7]. Dr Matthew Byrnes in my group is currently working with an OTTLE cell to study the spectroscopic properties of the oxidized radical cations.

In contrast to the starting materials, the bridged compounds are often intensely colored. For example, the oxalate bridged compound $[(^tBuCO_2)_3M_2]_2$(μ-O_2CCO_2) is red (M = Mo) and blue (M = W) and their respective higher oligomers obtained from Eq. (1) are maroon and almost black, respectively [3]. The room temperature electronic absorption spectra of the oxalate bridged 'dimers of dimers' supported by pivalate ligands are compared in Fig. 4. These intense absorptions were rightly assigned by Cayton as δ to oxalate π^* transitions and the red-shift observed for the tungsten compound owes its origin in the higher energy of the $W_2\delta$ orbitals, just as shown in Fig. 1.

With Professor Robin Clark and Dr Steven Firth at University College London, Dr Ann Macintosh started to examine the Raman and resonance Raman spectra of these bridged dinuclear complexes. With excitation wavelengths within the $M_2\delta$ to oxalate π^* transition, very strong resonance enhancement was seen for the $\nu_s(CO_2)$ stretching mode of the oxalate together with some enhancement of ν(CC). From ^{13}C labeling of the oxalate, it was clear that there was extensive coupling of all the symmetric modes of oxalate [9].

In collaboration with a colleague, Professor Jeffrey Zaleski, Dr Ann Macintosh and Dr Paul Wilson have reinvestigated the electronic spectra of the oxalate-bridged pivalate complexes in 2-methyltetraydrofuran as a function of temperature. Upon cooling, there is a notable bathochromic shift and at low temperatures, there is clear evidence of a vibronic progression. The electronic spectrum of the tungsten complex at 2 K in a 2MeTHF glass is shown in Fig. 5. The use of ^{13}C labeling in the oxalate identifies the primary progression as an oxalate-based vibrational mode [9].

The μ-O_2C–C_6F_4–CO_2 bridged compounds show very different colors in the solid-state and solution and a comparison of the mull spectrum with the solution spectrum recorded in THF at 25 °C, is shown in Fig. 6 for M = W. The low energy intense absorption at 900 nm is again reconcilable as $M_2\delta$ to bridge charge transfer and that this is at higher energy in the mull spectrum leads us to suggest that conjugation is greater in solution than it is in the solid-state. This, together with the temperature dependence of the oxalate bridged compounds, has led us to look further at the electronic structure of oxalate and perfluoroteraphthalate bridged M_2 complexes.

In collaboration with my colleagues Professor Bruce Bursten and Professor Christopher Hadad, Dr Paul Wilson has now completed computations employing density functional theory on the model compounds $[(HCO_2)_3M_2]_2$(μ-O_2CCO_2) and $[(HCO_2)_3M_2]_2$(μ-O_2C–C_6F_4–CO_2) for both M = Mo and W [13].

The electronic coupling arises from the interaction of the $M_2\delta$ in-and-out-of-phase combinations with the CO_2 π and π^* orbitals as shown in **VI** and **VII** below.

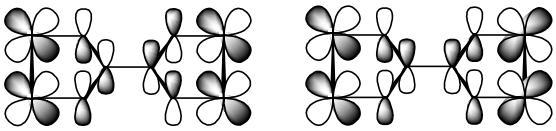

VI **VII**

In **VII**, the metals back-donate to the LUMO of the oxalate anion which is, as shown, C–O antibonding and C–C bonding. This stabilizes one δ combination. The other interaction is a filled-filled interaction and this leads to a destabilization of the other δ combination.

The optimized geometries indicate that the central $M_2(\mu$-$O_2CCO_2)M_2$ moiety is planar but the twisted D_{2d} geometry is only slightly higher in energy. Depending upon the method of calculation, GAUSSIAN98 or

ADF2000, we compute a barrier to rotation about the central oxalate C–C bond of 3–5 kcal mol^{-1}. The barrier is, however, consistently higher by ca. 3 kcal mol^{-1} for M = W as a result of the greater back-bonding interaction, **VII**.

An orbital energy diagram comparing the frontier orbitals of the $[(HCO_2)_3M_2]_2(\mu\text{-}O_2CCO_2)$ compounds, where M = Mo and W, is given in Fig. 7 and some of the key MO's are given in Fig. 8 using the plotting program GAUSSVIEW. The essential difference between the two complexes is the shift of the HOMO–LUMO gap to lower energy in going from Mo to W. The b_{2g} to b_{3u} transition is fully allowed, equivalent to metal-to-oxalate charge transfer. As can be seen in the orbital plot in Fig. 7, this increases the C–C bond order. The energy difference between the MO's that have mostly δ

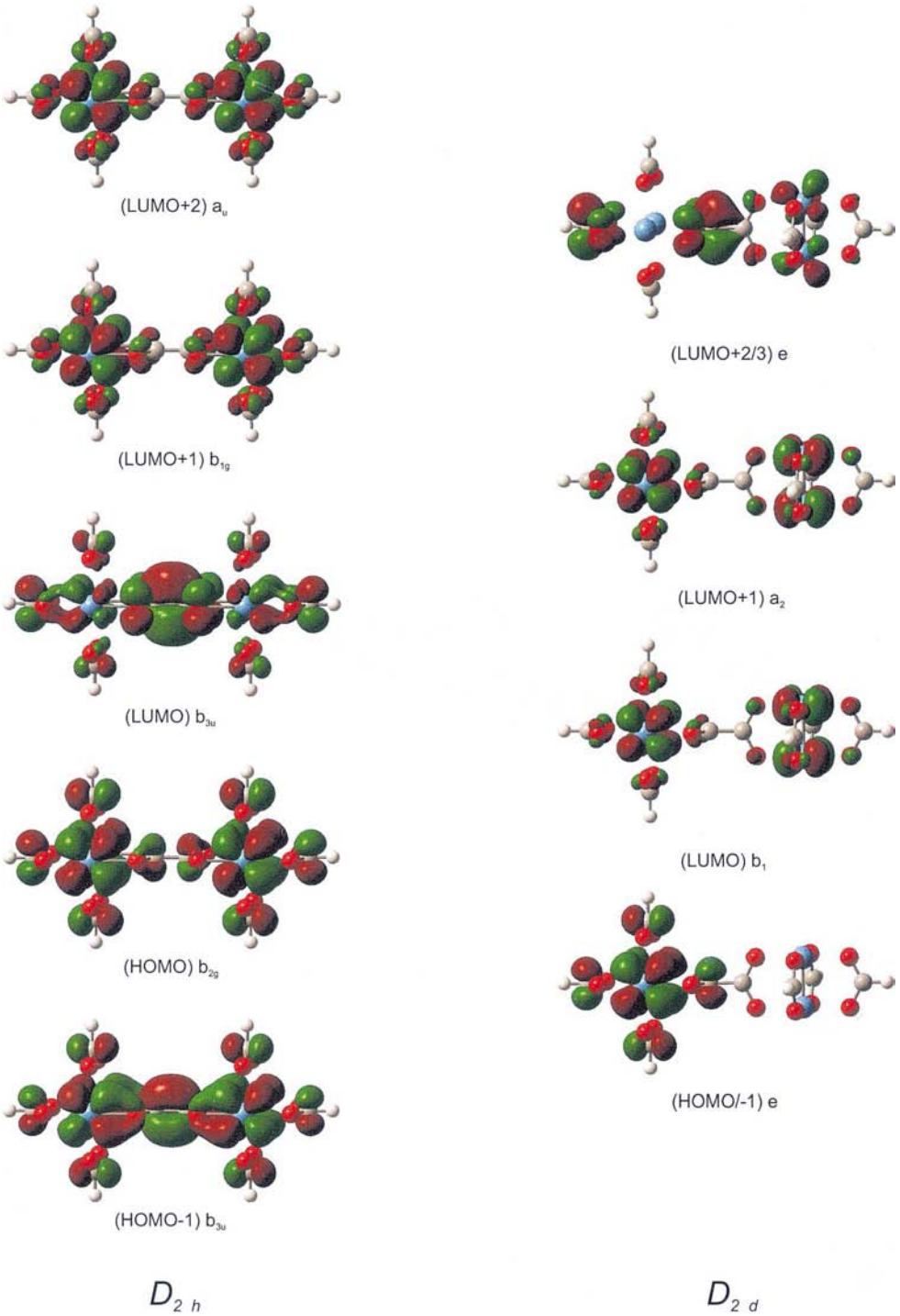

Fig. 8. Molecular orbital plots for some of the key frontier MOs in the $[Mo_2(O_2CH)_3]_2(\mu\text{-}O_2CCO_2)$ molecule in its planar (left) and twisted (right) forms.

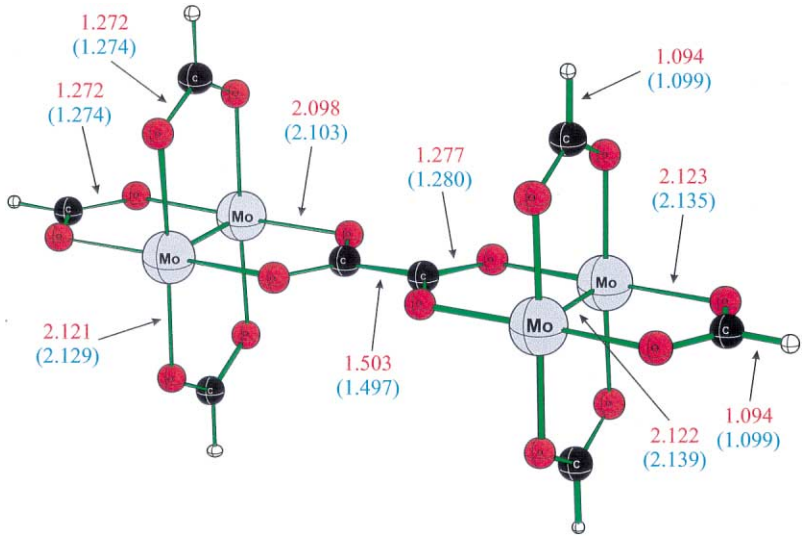

Fig. 9. View of the calculated metrical parameters for the D_{2h}-$[Mo_2(O_2CH)_3]_2(\mu\text{-}O_2CCO_2)$ molecule determined by GAUSSIAN. Results for the ADF calculations are given in parentheses.

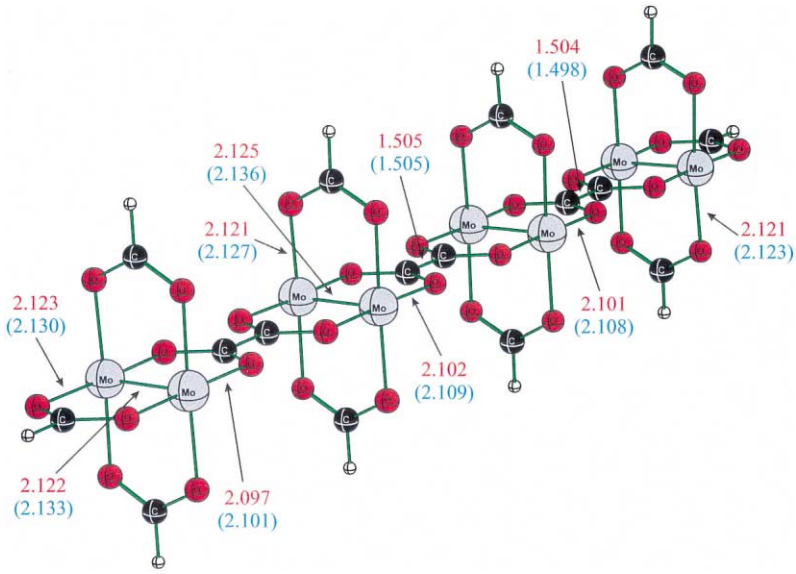

Fig. 10. Calculated metrical parameters for the linear $(HCO_2)_{10}Mo_8(\mu\text{-}O_2CCO_2)_3$ molecule as determined by GAUSSIAN. The ADF parameters are shown in parentheses.

character, the HOMO and HOMO-1, b_{2g} and b_{3u}, is nearly 0.5 eV for M = W, consistent with the strong coupling seen in the electrochemical data of the oxalate-bridged pivalate compound. The calculated and observed electronic transition energies for this allowed singlet b_{2g} to b_{3u} transition are in good agreement. The metrical parameters calculated for $[(HCO_2)_3M_2]_2(\mu\text{-}O_2CCO_2)$ also agree well with what would be expected based on the known structures of $Mo_2(O_2CR)_4$ compounds and the oxalate-bridged Mo_4 containing compounds characterized by Cotton and Murillo [5] (see Fig. 9).

The calculations on the perfluoroteraphthalate indicate a very small difference in energy between an all-planar structure and one where the Mo_2 units are perpendicular, ca. 2–3 kcal mol^{-1}. We believe that crystal packing forces favor a highly-twisted structure, one that does not favor $O_2C\text{–}C_6F_4\text{–}CO_2$ π conjugation in the solid-state. The LUMO of the bridging ligand thus becomes lower in energy in solution because of increased $O_2CC_6F_4CO_2$ conjugation resulting in the dramatic color changes [12].

Paul Wilson has also completed calculations on the model compounds $[(HCO_2)_2M_2(\mu\text{-}O_2CCO_2)]_4$, a cyclote-

tramer or molecular square, and a straight chain compound $(HCO_2)_{10}Mo_8(\mu\text{-}O_2CCO_2)_3$ (see Figs. 10 and 11). These calculations allow insight into the differences between the ring-compound, the molecular square, and a linear polymer of the same empirical formula $[(HCO_2)_2M_2(\mu\text{-}O_2CCO_2)]$.

In the square, the four sets of M_2 filled δ orbitals give rise to MO's of a_{1g}, e_u and b_{2g} symmetry in the D_{4h} point group. The a_{1g} and e_u orbitals are stabilized by back-bonding to oxalate while the HOMO is metal centered. The LUMO is oxalate C–C π with no metal mixing. Higher in energy are the set of four $M_2\delta^*$ combinations and oxalate-centered counterparts to the stabilized δ orbitals of a_{1g} and e_u symmetry. The splitting of $M_2\delta$ orbitals is calculated to be 0.7 eV for M = Mo and an orbital energy diagram is given in Fig. 12.

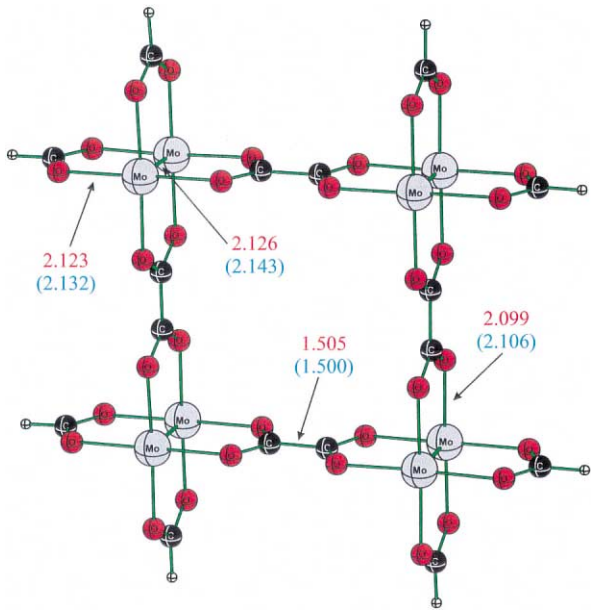

Fig. 11. Calculated metrical parameters for the D_{4h}-$[(HCO_2)_2Mo_2(\mu\text{-}O_2CCO_2)]_4$ molecule as determined by the GAUSSIAN and, in parentheses, the ADF packages.

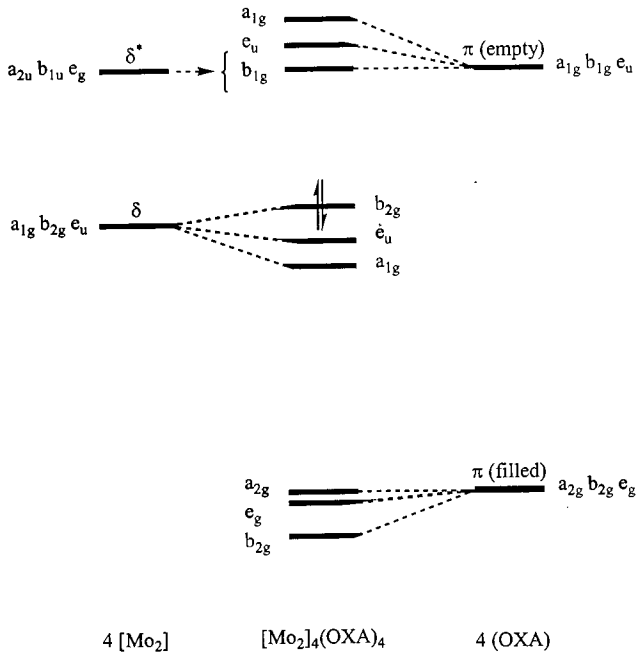

Fig. 12. Schematic MO energy level diagram for the frontier MOs of the D_{4h}-$[(HCO_2)_2Mo_2(\mu\text{-}O_2CCO_2)]_4$ molecule.

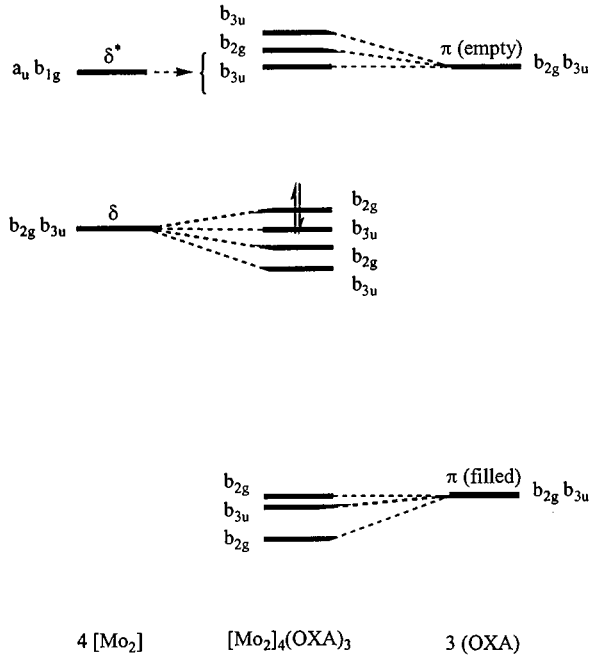

Fig. 13. Schematic MO energy level diagram for the D_{2h}-linear $(HCO_2)_{10}Mo_8(\mu\text{-}O_2CCO_2)_3$ molecule.

In the linear molecule, there are four M_2 units and three oxalates. In D_{2h} symmetry, we see the generation of $M_2\delta$'s of b_{2g} and b_{3u} symmetry. The interaction with the relevant three oxalate empty and filled orbitals leads to the orbital energy level diagram shown in Fig. 13. The key frontier molecular orbitals for the square and chain are shown in Fig. 14 [13].

From the comparison between the square and the chain, one can see an important difference. The HOMO–LUMO electronic transition is forbidden in the square but allowed in the chain. Indeed, for a linear chain polymer, we can see the emergence of a filled δ and an empty oxalate band for which E_{op}, the band gap will be notably smaller for tungsten than for molybdenum and, indeed, smaller than in the respective squares.

It should now be possible to return to some of the products formed in Eq. (1) and determine by a combination of physical techniques (solid-stated NMR, optical spectroscopy, X-ray powder pattern analysis) and computational procedures whether polymers or cyclotetramers are formed. Cotton and Murillo have recently reported the preparation of 'squares' of both Mo_2^{4+}

Rh_2^{4+} units supported by formamidinate ligands and oxalate or perfluoroteraphthalate bridges [14,15].

In closing, I should like to state that given the enormous variety of bridging ligands and the numerous possibilities in the selection of a dinuclear template, materials derived from covalently-linked M–M multiple bonds could have fascinating opto-electronic properties. But never fail to heed the words of the bard, ''Oft expectation fails and most oft there where most it promises'' [16].

It is surely enough challenge to make and characterize these fascinating compounds and not to sell them as stock options for future nanotechnologies.

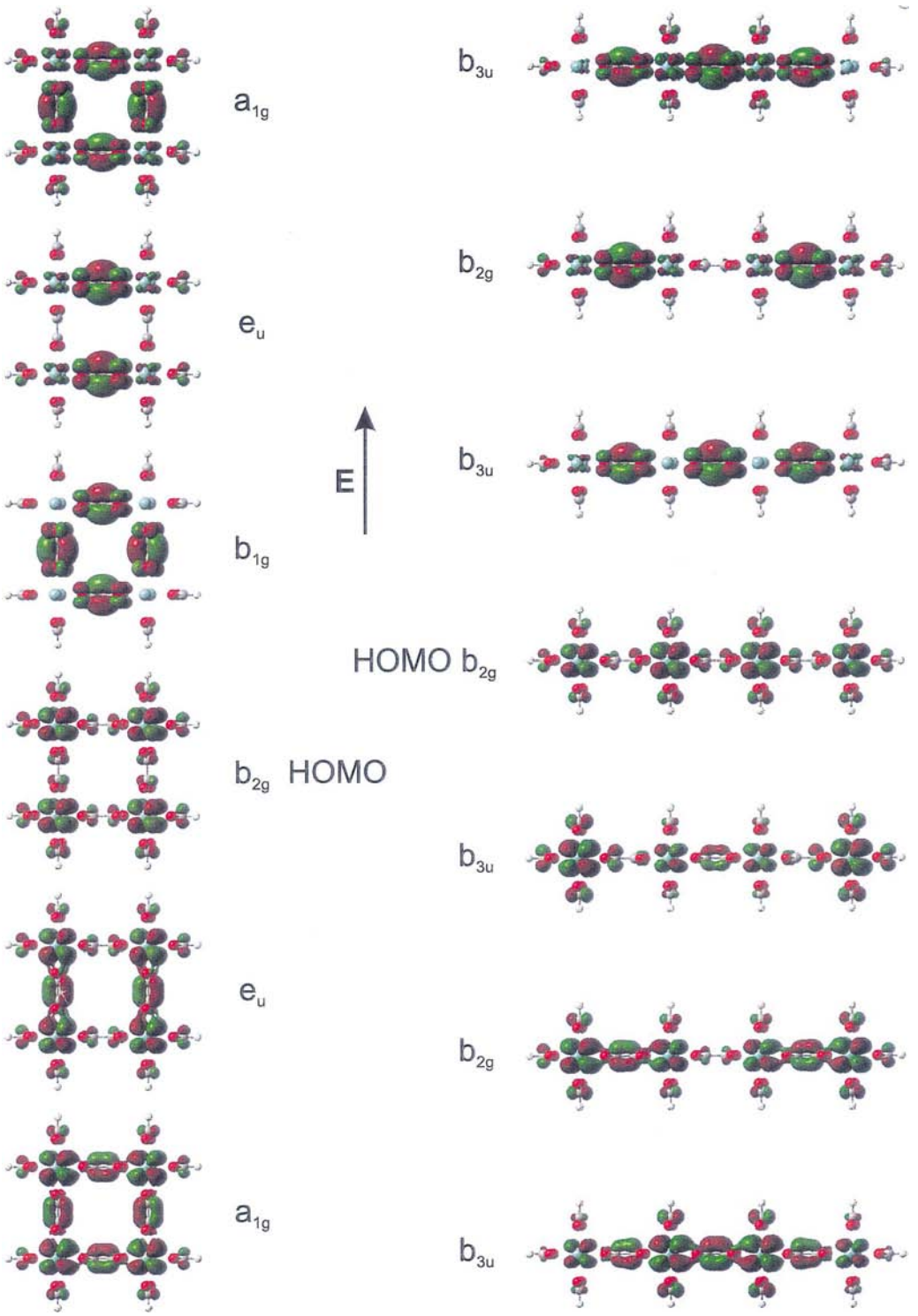

Fig. 14. Molecular orbital drawings of the key frontier MOs for the square and chain oxalate bridged Mo_8 containing complexes.

Acknowledgements

We thank the National Science Foundation for support of aspects of this work and the Ohio State Supercomputing Facility for computational resources. I am most grateful to my talented coworkers and colleagues who are cited in the references and text for bringing this project to its current position.

References

[1] F.A. Cotton, R.A. Walton, Multiple Bonds Between Metal Atoms, second ed., Oxford University Press, 1993.
[2] M.H. Chisholm, M.A. Lynn, Inorg. Chim. Acta 243 (1996) 283.
[3] R.H. Cayton, M.H. Chisholm, J.C. Huffman, E.B. Lobkovsky, J. Am. Chem. Soc. 113 (1991) 8709.
[4] M.H. Chisholm, A.M. Macintosh, J. Chem. Soc. Dalton Trans. (1999) 1205.
[5] F.A. Cotton, C. Lin, C.A. Murillo, J. Chem. Soc. Dalton Trans. (1998) 3151.
[6] F.A. Cotton, C. Lin, C.A. Murillo, Inorg. Chem. 40 (2001) 472.
[7] F.A. Cotton, J.P. Donahue, C. Lin, C.A. Murillo, Inorg. Chem. 40 (2001) 1234.
[8] M.H. Chisholm, P.J. Wilson, P.M. Woodward, results to be published.
[9] B.E. Bursten, M.H. Chisholm, R.J.H. Clark, S. Firth, C.M. Hadad, C.D. Hamilton, P.J. Wilson, J.M. Zaleski, J. Am. Chem. Soc., submitted.
[10] M.B. Robin, P. Day, Adv. Inorg. Radiochem. 10 (1967) 247.
[11] C. Creutz, Prog. Inorg. Chem. 30 (1983) 1.
[12] M.H. Chisholm, P.J. Wilson, results to be published.
[13] B.E. Bursten, M.H. Chisholm, C.M. Hadad, P.J. Wilson, Chem. Commun. (2001) 2382.
[14] F.A. Cotton, L.M. Daniels, C. Lin, C.A. Murillo, J. Am. Chem. Soc. 121 (1999) 4538.
[15] F.A. Cotton, C. Lin, C.A. Murillo, Inorg. Chem. 40 (2001) 478.
[16] W. Shakespeare, All's Well That Ends Well, II, *i*, pp. 145–146.